












# TECH BRIEFS

NATIONAL AERONAUTICS AND SPACE ADMINISTRATION

-  **Technology Focus**
-  **Computers/Electronics**
-  **Software**
-  **Materials**
-  **Mechanics**
-  **Machinery/Automation**
-  **Manufacturing**
-  **Bio-Medical**
-  **Physical Sciences**
-  **Information Sciences**
-  **Books and Reports**



## INTRODUCTION

Tech Briefs are short announcements of innovations originating from research and development activities of the National Aeronautics and Space Administration. They emphasize information considered likely to be transferable across industrial, regional, or disciplinary lines and are issued to encourage commercial application.

### Availability of NASA Tech Briefs and TSPs

Requests for individual Tech Briefs or for Technical Support Packages (TSPs) announced herein should be addressed to

#### National Technology Transfer Center

Telephone No. (800) 678-6882 or via World Wide Web at [www2.nttc.edu/leads/](http://www2.nttc.edu/leads/)

Please reference the control numbers appearing at the end of each Tech Brief. Information on NASA's Commercial Technology Team, its documents, and services is also available at the same facility or on the World Wide Web at [www.nctn.hq.nasa.gov](http://www.nctn.hq.nasa.gov).

Commercial Technology Offices and Patent Counsels are located at NASA field centers to provide technology-transfer access to industrial users. Inquiries can be made by contacting NASA field centers and program offices listed below.

## NASA Field Centers and Program Offices

#### Ames Research Center

Carolina Blake  
(650) 604-1754  
[cblake@mail.arc.nasa.gov](mailto:cblake@mail.arc.nasa.gov)

#### Dryden Flight Research Center

Jenny Baer-Riedhart  
(661) 276-3689  
[jenny.baer-riedhart@dfrc.nasa.gov](mailto:jenny.baer-riedhart@dfrc.nasa.gov)

#### Goddard Space Flight Center

Nona Cheeks  
(301) 286-5810  
[Nona.K.Cheeks.1@gsfc.nasa.gov](mailto:Nona.K.Cheeks.1@gsfc.nasa.gov)

#### Jet Propulsion Laboratory

Art Murphy, Jr.  
(818) 354-3480  
[arthur.j.murphy-jr@jpl.nasa.gov](mailto:arthur.j.murphy-jr@jpl.nasa.gov)

#### Johnson Space Center

Charlene E. Gilbert  
(281) 483-3809  
[commercialization@jsc.nasa.gov](mailto:commercialization@jsc.nasa.gov)

#### Kennedy Space Center

Jim Aliberti  
(321) 867-6224  
[Jim.Aliberti-1@ksc.nasa.gov](mailto:Jim.Aliberti-1@ksc.nasa.gov)

#### Langley Research Center

Sam Morello  
(757) 864-6005  
[s.a.morello@larc.nasa.gov](mailto:s.a.morello@larc.nasa.gov)

#### John H. Glenn Research Center at Lewis Field

Larry Viterna  
(216) 433-3484  
[cto@grc.nasa.gov](mailto:cto@grc.nasa.gov)

#### Marshall Space Flight Center

Vernotto McMillan  
(256) 544-2615  
[vernotto.mcmillan@msfc.nasa.gov](mailto:vernotto.mcmillan@msfc.nasa.gov)

#### Stennis Space Center

Robert Bruce  
(228) 688-1929  
[robert.c.bruce@nasa.gov](mailto:robert.c.bruce@nasa.gov)

#### NASA Program Offices

At NASA Headquarters there are seven major program offices that develop and oversee technology projects of potential interest to industry:

#### Carl Ray

Small Business Innovation Research Program (SBIR) & Small Business Technology Transfer Program (STTR)  
(202) 358-4652 or  
[cray@mail.hq.nasa.gov](mailto:cray@mail.hq.nasa.gov)

#### Dr. Robert Norwood

Office of Commercial Technology (Code RW)  
(202) 358-2320 or  
[rnorwood@mail.hq.nasa.gov](mailto:rnorwood@mail.hq.nasa.gov)

#### John Mankins

Office of Space Flight (Code MP)  
(202) 358-4659 or  
[jmankins@mail.hq.nasa.gov](mailto:jmankins@mail.hq.nasa.gov)

#### Terry Hertz

Office of Aero-Space Technology (Code RS)  
(202) 358-4636 or  
[thertz@mail.hq.nasa.gov](mailto:thertz@mail.hq.nasa.gov)

#### Glen Mucklow

Office of Space Sciences (Code SM)  
(202) 358-2235 or  
[gmucklow@mail.hq.nasa.gov](mailto:gmucklow@mail.hq.nasa.gov)

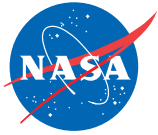
#### Roger Crouch

Office of Microgravity Science Applications (Code U)  
(202) 358-0689 or  
[rcrouch@hq.nasa.gov](mailto:rcrouch@hq.nasa.gov)

#### Granville Paules

Office of Mission to Planet Earth (Code Y)  
(202) 358-0706 or  
[gpaules@mtpe.hq.nasa.gov](mailto:gpaules@mtpe.hq.nasa.gov)





# TECH BRIEFS

NATIONAL AERONAUTICS AND SPACE ADMINISTRATION



## 5 Technology Focus: Fastening/Joining/Assembly Technologies

- 5 Tool for Bending a Metal Tube Precisely in a Confined Space
- 6 Multiple-Use Mechanisms for Attachment to Seat Tracks
- 7 Force-Measuring Clamps
- 7 Cellular Pressure-Actuated Joint



## 9 Computers/Electronics

- 9 Block QCA Fault-Tolerant Logic Gates
- 10 Hybrid VLSI/QCA Architecture for Computing FFTs
- 11 Arrays of Carbon Nanotubes as RF Filters in Waveguides
- 12 Carbon Nanotubes as Resonators for RF Spectrum Analyzers



## 15 Software

- 15 Software for Viewing Landsat Mosaic Images
- 15 Updated Integrated Mission Program
- 15 Software for Sharing and Management of Information
- 15 Update on Integrated Optical Design Analyzer



## 17 Materials

- 17 Optical-Quality Thin Polymer Membranes



## 19 Mechanics

- 19 Rollable Thin Shell Composite-Material Paraboloidal Mirrors
- 19 Folded Resonant Horns for Power Ultrasonic Applications



## 21 Machinery/Automation

- 21 Touchdown Ball-Bearing System for Magnetic Bearings
- 22 Flux-Based Deadbeat Control of Induction-Motor Torque



## 23 Manufacturing

- 23 Block Copolymers as Templates for Arrays of Carbon Nanotubes



## 25 Physical Sciences

- 25 Throttling Cryogen Boiloff To Control Cryostat Temperature



## 27 Information Sciences

- 27 Collaborative Software Development Approach Used to Deliver the New Shuttle Telemetry Ground Station



## 29 Books and Reports

- 29 Turbulence in Supercritical O<sub>2</sub>/H<sub>2</sub> and C<sub>7</sub>H<sub>16</sub>/N<sub>2</sub> Mixing Layers
- 29 Time-Resolved Measurements in Optoelectronic Microbioanalysis

This document was prepared under the sponsorship of the National Aeronautics and Space Administration. Neither the United States Government nor any person acting on behalf of the United States Government assumes any liability resulting from the use of the information contained in this document, or warrants that such use will be free from privately owned rights.





## ⊕ Tool for Bending a Metal Tube Precisely in a Confined Space

This tool offers capabilities that prior tools do not.

*Goddard Space Flight Center, Greenbelt, Maryland*

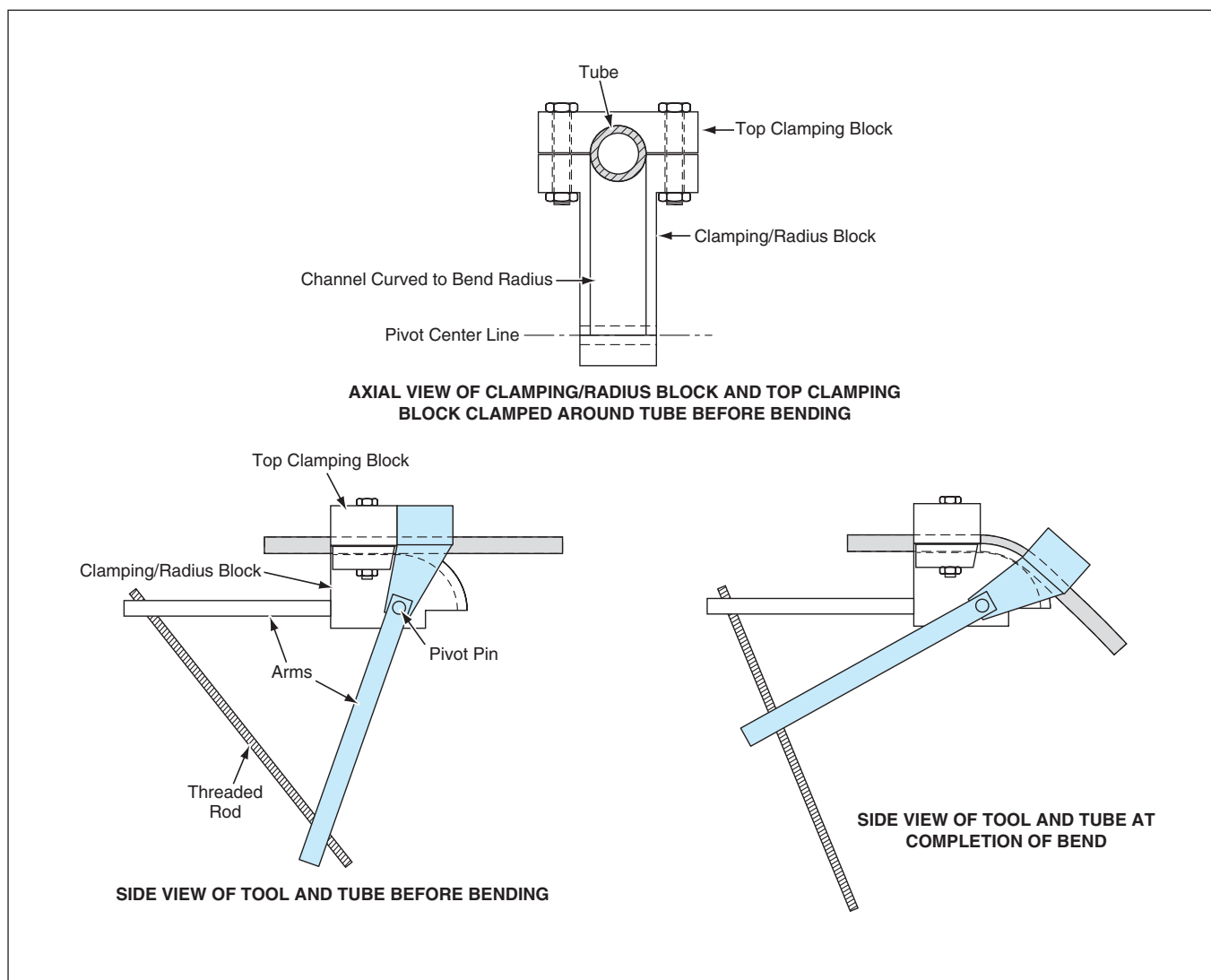
A relatively simple, manually operated tool enables precise bending (typically, within  $\pm 1/2^\circ$  of the specified bend angle) of a metal tube located in a confined space, with a minimum of flattening of the tube and without significant gouging of the tube surface. The tool is designed for use in a situation in which the tube cannot be removed from the confined space for placement in a conventional bench-mounted tube bender. The tool is also designed for use in a situation in which previously available hand-held tube

benders do not afford the required precision, do not support the tube wall sufficiently to prevent flattening or gouging, and/or do not fit within the confined space.

The tool is designed and fabricated for the specific outer diameter and bend radius of the tube to be bent. The tool (see figure) includes a clamping/radius block and a top clamping block that contain mating straight channels of semicircular cross section that fit snugly around the tube. The mating portions of the clamping/radius block and the top

clamping block are clamped around a length of the tube that is adjacent to the bend and that is intended to remain straight. The clamping/radius block is so named because beyond the straight clamping section, its semicircular channel extends to a non-clamping section that is curved at the specified bend radius. A pivot hole is located in the clamping/radius block at the center of the bend circle.

The tool includes a bending block that, like the other blocks, contains a straight semicircular channel that fits



A Tube Is Clamped and Bent in contact with conformal tubelike surfaces that provide full support with minimal damage.

around the outside of the tube. The bending block contains a pivot hole to be aligned with the pivot hole in the clamping/radius block. Once the tube has been clamped between the clamping/radius and top clamping blocks, the bending block is placed around the tube, the pivot holes are aligned, and a pivot pin is inserted through the pivot holes.

To bend the tube, the bending block is pivoted so that its semicircular groove slides along the tube, forcing the tube into the curved portion of the

groove in the clamping/radius block. An arm that extends from the clamping/radius block and a similar arm that extends from the bending block provide mechanical advantage for generating bending torques and forces. These arms are actuated by turning a nut on a threaded rod that runs through holes in both arms.

To ensure a precise bend, one should measure the bend angle by use of a protractor at intervals during the bending operation. Even so, it is desirable to calibrate the tool in two ways: (1) measur-

ing and/or calculating the increase in the bend angle for each turn of the nut and (2) measuring and/or calculating the amount of springback. Calibration should facilitate the approach to the final stage of bending (with a slight over-bend to allow for springback) with greater assurance that at the end, the tube will be bent to the desired angle within  $\pm 1/2^\circ$ .

*This work was done by Gary T. Davis of Goddard Space Flight Center. Further information is contained in a TSP (see Page 1). GSC-14412*

## Multiple-Use Mechanisms for Attachment to Seat Tracks

These could serve as standard or universal seat-track clamps.

*Lyndon B. Johnson Space Center, Houston, Texas*

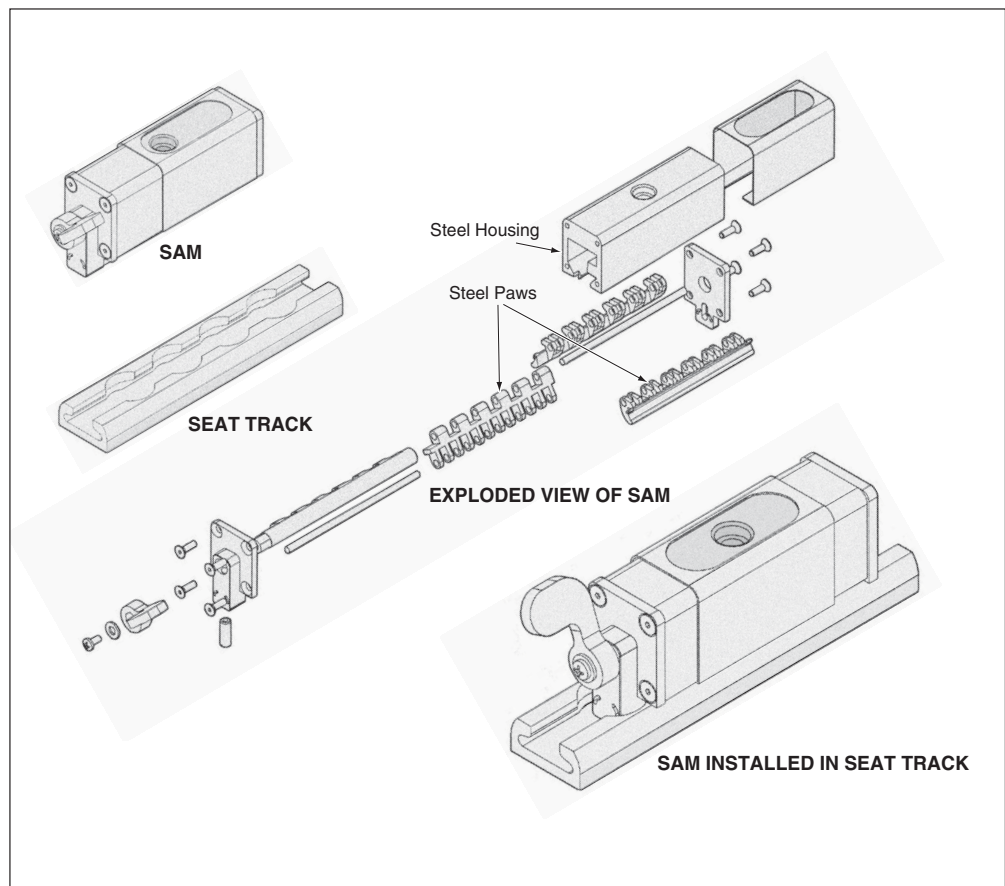
A Seat Track Attach Mechanism (SAM) is a multiple-use clamping device intended for use in mounting various objects on the standard seat tracks used on the International Space Station (ISS). The basic SAM design could also be adapted to other settings in which seat tracks are available: for example, SAM-like devices could be used as universal aircraft-seat-track mounting clamps.

A SAM (see figure) is easily installed by inserting it in a seat track, then actuating a locking lever to clamp the SAM to the track. The SAM includes an over-center locking feature that prevents premature disengagement that could be caused by some inadvertent movements of persons or objects in the vicinity.

A SAM can be installed in, or removed from, any position along a seat track, without regard for the locations of the circular access holes. Hence, one or more SAM(s) can be used to mount an object or objects on a track or a pair of tracks in an infinite number of preferred configurations. A SAM can be incorporated into a dual swivel device, so that two of the SAMs can be made to lock onto two side-by-side seat tracks simultaneously, as would be the case in a standard ISS rack bay where two side-by-side racks reside. The main benefit to

using two SAMs in a side-by-side arrangement is to provide a coupled load. By picking up load points on two seat tracks, a coupled loading is created, improving the stability and strength since the load is spread to two seat tracks at a short distance.

*This work was done by Martin Fraske and Rich May of Johnson Engineering Corp. for Johnson Space Center. For further information, contact the Johnson Commercial Technology Office at 281-483-3809; commercialization@jsc.nasa.gov. MSC-23299*



A SAM is Inserted in, and Clamps Onto, a Seat Track. The SAM can be positioned anywhere along the track, without regard for the locations of the access holes.



---

## Force-Measuring Clamps

**Clamping forces can be measured easily and quickly.**

*Dryden Flight Research Center, Edwards, California*

Force-measuring clamps have been invented to facilitate and simplify the task of measuring the forces or pressures applied to clamped parts. There is a critical need to measure clamping forces or pressures in some applications — for example, while bonding sensors to substrates or while clamping any sensitive or delicate parts. Many manufacturers of adhesives and sensors recommend clamping at specific pressures while bonding sensors or during adhesive bonding between parts in general.

In the absence of a force-measuring clamp, measurement of clamping force can be cumbersome at best because of the need for additional load sensors and load-indicating equipment. One prior method of measuring clamping force involved the use of load washers or miniature load cells in combination with external power sources and load-indicating equipment. Calibrated spring clamps have also been used. Load washers and miniature load cells constitute additional clamped parts in load paths and can add to the destabilizing effects of loading mechanisms. Spring clamps can lose calibration quickly through weakening of the springs and are limited to the maximum forces that the springs can apply.

The basic principle of a force-measuring clamp can be implemented on a clamp of almost any size and can enable measurement of a force of almost any magnitude. No external equipment is

needed because the component(s) for transducing the clamping force and the circuitry for supplying power, conditioning the output of the transducers, and displaying the measurement value are all housed on the clamp. In other words, a force-measuring clamp is a complete force-application and force-measurement system all in one package. The advantage of unitary packaging of such a system is that it becomes possible to apply the desired clamping force or pressure with precision and ease.

Like many other load-measuring devices, a force-measuring clamp contains strain gauges and exploits the well-known proportionality between strain and applied force or pressure. More specifically, a force-measuring clamp contains four strain gauges electrically connected in a Wheatstone bridge. The bridge output is fed to zero and span circuitry, the output of which is digitized and displayed. The span and zero circuitry make it possible to calibrate the bridge output to indicate force or pressure in any suitable unit of measure.

The strain gauges can be installed by use of Measurements Group M-Bond 610 (or equivalent) epoxy-phenolic adhesive or Measurements Group AE 10 (or equivalent) epoxy adhesive. The strain gauges are connected to a terminal strip for incorporation into the bridge by wires of 34 American Wire Gauge [ $\approx 6.3$  mils ( $\approx 0.16$  mm) in diameter]. Wires of the same size

are used for connections between the terminal and a printed-circuit board. The printed-circuit board contains a voltage-regulation circuit, the span and zero circuits, two watch batteries, and a power switch. The final-stage output of the printed circuit is fed to a digital-display device that is plugged into the printed-circuit board, and is controlled by the zero and span circuits. Operation of the force-measuring clamp is easy: One simply slides the power switch to “on,” adjusts the display to zero if necessary, applies a clamping force, and reads the display.

The functionality of a “breadboard” prototype force-measuring clamp was tested in a laboratory by use of the combination of certified weights, a load washer, a strain indicator, and a voltmeter. Some alternate or future embodiments of force-measuring clamps may include smaller batteries and/or smaller digital displays for the sake of compactness, more options, and better packaging of all components. Force-measuring clamps and/or similar devices could also be incorporated into other mechanisms.

*This work was done by Mark Nunnelee of Dryden Flight Research Center.*

*This invention has been patented by NASA (patent pending). Inquiries concerning nonexclusive or exclusive license for its commercial development should be addressed to Yvonne Kellogg, Technology Commercialization Specialist, Dryden Flight Research Center, (661)276-3720. Refer to DRC-99-37.*

---

## Cellular Pressure-Actuated Joint

**Pockets in one of the sealing members would help maintain differential pressure.**

*Marshall Space Flight Center, Alabama*

A modification of a pressure-actuated joint has been proposed to improve its pressure actuation in such a manner as to reduce the potential for leakage of the pressurizing fluid. The specific joint for which the modification is proposed is a field joint in a reusable solid-fuel rocket motor (RSRM), in which the pressurizing fluid is a mixture of hot combustion gases. The proposed modification could also be applicable to other pressure-actuated joints of similar configuration.

The RSRM field joint (see figure) includes a pressure-actuated member denoted the J-leg, which is part of a body of insulation. A pressure-sensitive adhesive (PSA) is used to bond the sealing surface of the J-leg to the sealing surface of another body of insulation. The pressure actuation is supposed to push these two sealing surfaces together. However, experience with the joint indicates that it may not behave as a truly pressure-actuated system.

The modified version of the joint would be the same as the unmodified version, except that pockets of empty volume would be introduced into the body against which the J-leg is pressed. The size, shape, and orientation of the pockets would be such upon the application of pressure to the hot-gas side of the J-leg, the volumes of the pockets would not change significantly and hence the pressures in the pockets, would not change significantly; the net result would be that the pockets would support

the buildup of enough differential pressure across the J-leg so that the joint would behave more nearly like a truly pressure-actuated system.

The breakup of the empty volume into multiple pockets would counteract the tendency toward leakage that would be incurred by introducing a single

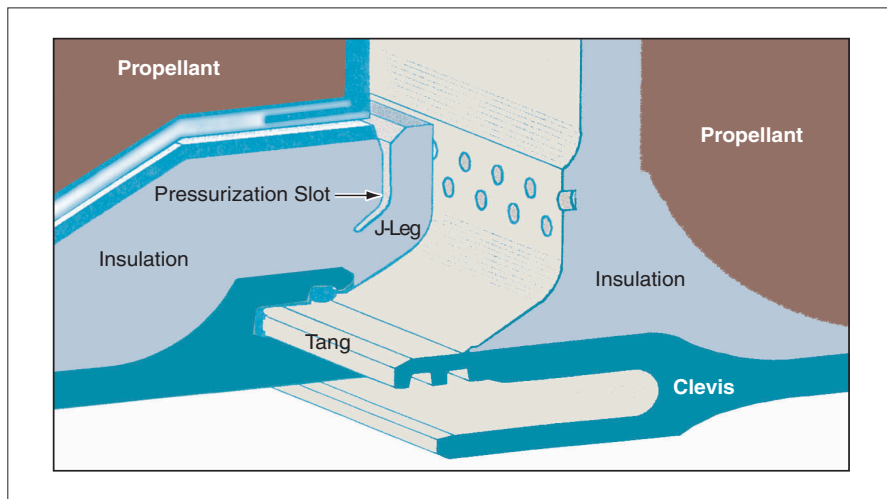
larger pocket. In the unlikely event that a gas path penetrated the joint, only one pocket would be compromised, while the others would continue to maintain the differential pressure needed for pressure actuation.

*This work was done by John R. McGuire of Thiokol Propulsion for Marshall Space Flight Center.*

*Title to this invention has been waived under the provisions of the National Aeronautics and Space Act {42 U.S.C. 2457(f)} to Thiokol Propulsion. Inquiries concerning licenses for its commercial development should be addressed to*

*Thiokol Propulsion  
PO Box 707  
Brigham City, UT 84302-0707  
Tel. No.: (435) 863-3511  
Fax No.: (435) 863-2234*

*Refer to MFS-31652, volume and number of this NASA Tech Briefs issue, and the page number.*



The **Modified RSRM Field Joint** would be the same as the unmodified one, except for the introduction of the pockets.



## Block QCA Fault-Tolerant Logic Gates

It may become possible to relax manufacturing tolerances in molecular-scale devices.

NASA's Jet Propulsion Laboratory, Pasadena, California

Suitably patterned arrays (blocks) of quantum-dot cellular automata (QCA) have been proposed as fault-tolerant universal logic gates. These block QCA gates could be used to realize the potential of QCA for further miniaturization, reduction of power consumption, increase in switching speed, and increased degree of integration of very-large-scale integrated (VLSI) electronic circuits.

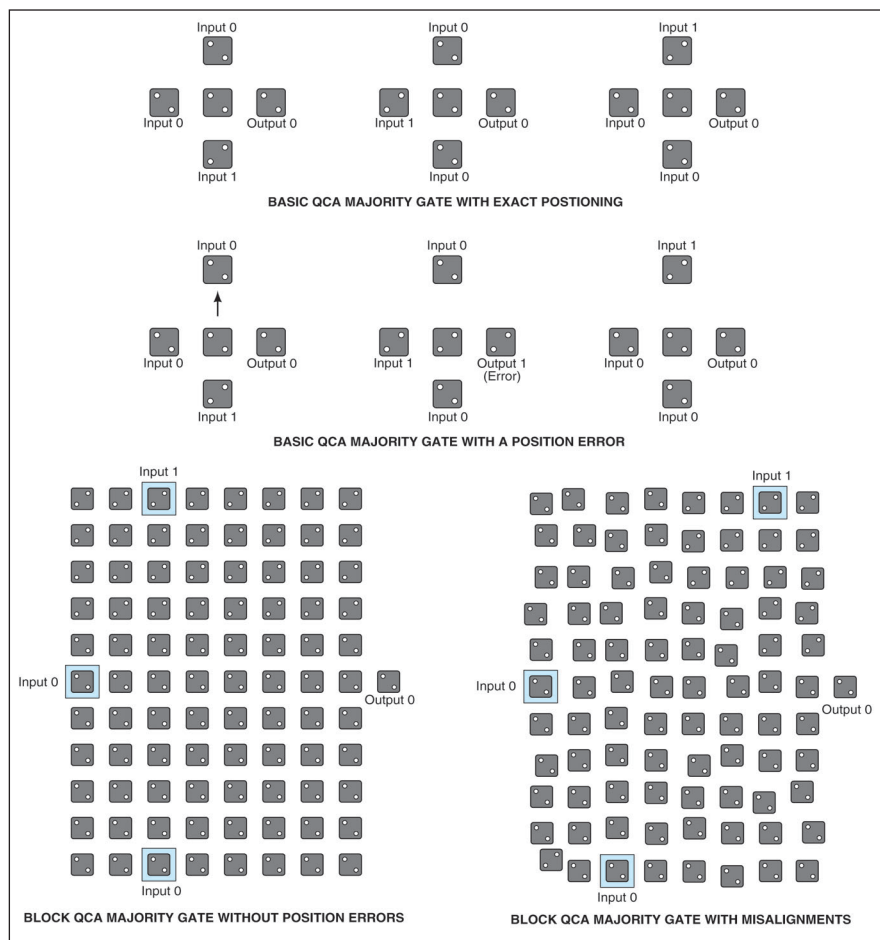
The limitations of conventional VLSI circuitry, the basic principle of operation of QCA, and the potential advantages of QCA-based VLSI circuitry were described in several *NASA Tech Briefs* articles, namely "Implementing Permutation Matrices by Use of Quantum Dots" (NPO-20801),

Vol. 25, No. 10 (October 2001), page 42; "Compact Interconnection Networks Based on Quantum Dots" (NPO-20855) Vol. 27, No. 1 (January 2003), page 32; "Bit-Serial Adder Based on Quantum Dots" (NPO-20869), Vol. 27, No. 1 (January 2003), page 35; and "Hybrid VLSI/QCA Architecture for Computing FFTs" (NPO-20923), which follows this article. To recapitulate the principle of operation (greatly oversimplified because of the limitation on space available for this article): A quantum-dot cellular automata contains four quantum dots positioned at or between the corners of a square cell. The cell contains two extra mobile electrons that can tunnel (in the quantum-

mechanical sense) between neighboring dots within the cell. The Coulomb repulsion between the two electrons tends to make them occupy antipodal dots in the cell. For an isolated cell, there are two energetically equivalent arrangements (denoted polarization states) of the extra electrons. The cell polarization is used to encode binary information. Because the polarization of a nonisolated cell depends on Coulomb-repulsion interactions with neighboring cells, universal logic gates and binary wires could be constructed, in principle, by arraying QCA in suitable design in suitable patterns.

Heretofore, researchers have recognized two major obstacles to realization of QCA-based logic gates: One is the need for (and the difficulty of attaining) operation of QCA circuitry at room temperature or, for that matter, at any temperature above a few Kelvins. It has been theorized that room-temperature operation could be made possible by constructing QCA as molecular-scale devices. However, in approaching the lower limit of miniaturization at the molecular level, it becomes increasingly imperative to overcome the second major obstacle, which is the need for (and the difficulty of attaining) high precision in the alignments of adjacent QCA in order to ensure the correct interactions among the quantum dots.

The fault-tolerant logic gates that would be implemented by blocks of QCA according to the proposal include majority and inverter (NOT) gates, which are said to be universal logic gates because other logic gates (AND, OR, and NOR) can be implemented as combinations of majority and inverter gates. The figure depicts examples of (1) a basic QCA majority gate manufactured with exact positioning of all QCA, (2) a basic QCA majority gate manufactured with a significant position error, (3) a block QCA gate manufactured with exact positioning, and (4) a block QCA gate manufactured with irregularity of positions in the QCA array and errors in the choice of the edge QCAs used for input. These and other examples were analyzed by computational simulation, using a program developed at the University of Notre



Basic and Block QCA Majority Gates, with and without misalignments, were analyzed by computational simulation. The results of the analysis showed that, relative to the basic gate, the block gate would be more tolerant of manufacturing errors.

Dame, that implements a Hartree-Fock mathematical model of the physics of a QCA array. The simulation was performed for an assumed cell size of 20 nm and inter-cell distance of 14 nm.

The results of the simulation showed that for a basic QCA majority gate, an output error would occur if the errors in the relative positions of adjacent cells were to exceed various amounts of the order of the size of a cell or a significant fraction thereof (the exact amounts being different for different cells and different directions of displacement).

In the case of a molecular implementation, this would translate to a requirement for impractical sub-nanometer manufacturing tolerances. On the other hand, the simulation showed that even with errors as large as those depicted for the block majority gate at the bottom of the figure, there would be no output error.

*This work was done by Amir Firjany, Nikzad Toomarian, and Katayoon Modarres of Caltech for NASA's Jet Propulsion Laboratory. Further information is contained in a TSP (see Page 1).*

*In accordance with Public Law 96-517, the contractor has elected to retain title to this invention. Inquiries concerning rights for its commercial use should be addressed to*

*Intellectual Property group*

*JPL*

*Mail Stop 202-233*

*4800 Oak Grove Drive*

*Pasadena, CA 91109*

*(818) 354-2240*

*Refer to NPO-21127, volume and number of this NASA Tech Briefs issue, and the page number.*

## Hybrid VLSI/QCA Architecture for Computing FFTs

Simplification is effected through use of QCA circuitry to permute data.

NASA's Jet Propulsion Laboratory, Pasadena, California

A data-processor architecture that would incorporate elements of both conventional very-large-scale integrated (VLSI) circuitry and quantum-dot cellular automata (QCA) has been proposed to enable the highly parallel and systolic computation of fast Fourier transforms (FFT). The proposed circuit would complement the QCA-based circuits described in several prior NASA Tech Briefs articles, namely "Implementing Permutation Matrices by Use of Quantum Dots" (NPO-20801), Vol. 25, No. 10 (October 2001), page 42; "Compact Interconnection Networks Based on Quantum Dots" (NPO-20855) Vol. 27, No. 1 (January 2003), page 32; and "Bit-Serial Adder Based on Quantum Dots" (NPO-20869), Vol. 27, No. 1 (January 2003), page 35.

The cited prior articles described the limitations of very-large-scale integrated (VLSI) circuitry and the major potential advantage afforded by QCA. To recapitulate: In a VLSI circuit, signal paths that are required not to interact with each other must not cross in the same plane. In contrast, for reasons too complex to describe in the limited space available for this article, suitably designed and operated QCA-based signal paths that are required not to interact with each other can nevertheless be allowed to cross each other in the same plane without adverse effect. In principle, this characteristic could be exploited to design compact, coplanar, simple (relative to VLSI) QCA-based networks to implement complex, advanced interconnection schemes.

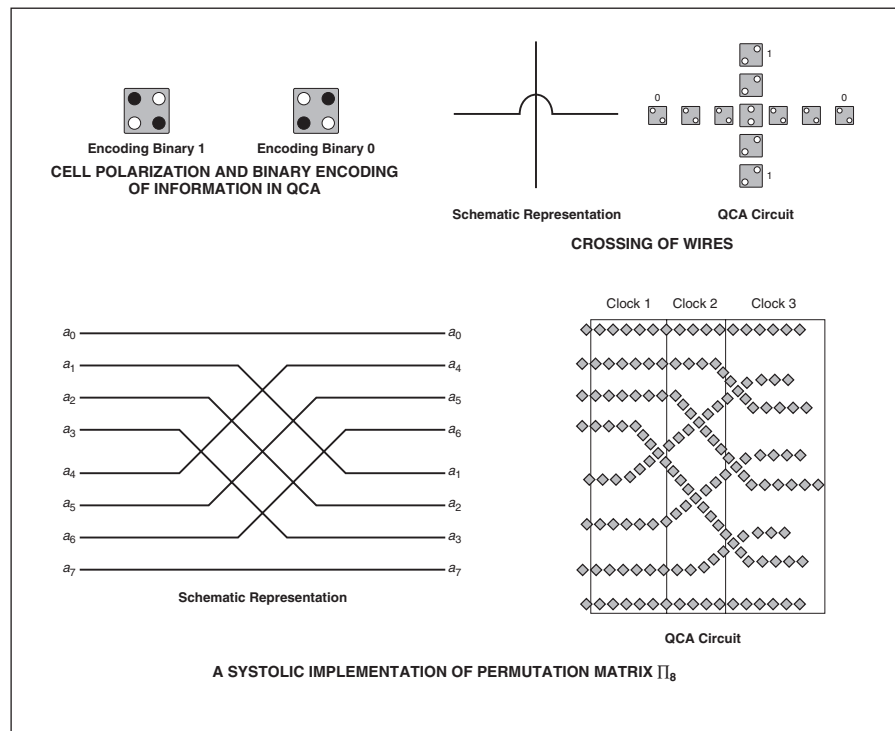


Figure 1. QCA Are Assembled Into Binary Wires, and the wires are patterned to implement a perfect-shuffle permutation matrix known as  $\Pi_8$ .

To enable a meaningful description of the proposed FFT-processor architecture, it is necessary to further recapitulate the description of a quantum-dot cellular automaton from the first-mentioned prior article: A quantum-dot cellular automaton contains four quantum dots positioned at or between the corners of a square cell. The cell contains two extra mobile electrons that can tunnel (in the quantum-mechanical sense) between neighboring

dots within the cell. The Coulomb repulsion between the two electrons tends to make them occupy antipodal points in the cell. For an isolated cell, there are two energetically equivalent arrangements (denoted polarization states) of the extra electrons. The cell polarization is used to encode binary information. Because the polarization of a nonisolated cell depends on Coulomb-repulsion interactions with neighboring cells, universal logic gates

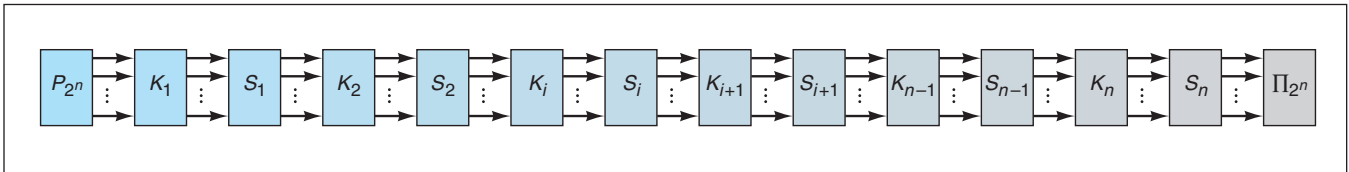


Figure 2. A Hybrid of VLSI and QCA Circuit Modules would perform a parallel, systolic computation of an FFT. The particular circuit architecture is based on a matrix factorization of the FFT.

and binary wires could be constructed, in principle, by arraying QCA of suitable design in suitable patterns.

Again, for reasons too complex to describe here, in order to ensure accuracy and timeliness of the output of a QCA array, it is necessary to resort to an adiabatic switching scheme in which the QCA array is divided into subarrays, each controlled by a different phase of a multiphase clock signal. In this scheme, each subarray is given time to perform its computation, then its state is frozen by raising its interdot potential barriers and its output is fed as the input to the successor subarray. The successor subarray is kept in an unpolarized state so it does not influence the calculation of preceding subarray. Such a clocking scheme is consistent with pipeline computation in the sense that each different subarray can perform a different part of an overall computation. In other words, QCA arrays are inherently suitable for pipeline and, moreover, systolic computations. This sequential or pipeline aspect of QCA would be utilized in the proposed FFT-processor architecture.

Heretofore, the main obstacle to de-

signing VLSI circuits for systolic and highly parallel computation of FFTs (and of other fast transforms commonly used in the processing of images and signals) has been the need for complex data permutations that cannot be implemented without crossing of signal paths. The proposed hybrid VLSI/QCA FFT-processor architecture would exploit the coplanar-signal-path-crossing capability of QCA to implement the various permutations directly in patterns of binary wires (that is, linear arrays of quantum dots), as in the example of Figure 1. The proposed architecture is based on a reformulation of the FFT by use of a particular matrix factorization that is suitable for systolic implementation. The reformulated FFT is given by

$$F_{2^n} = \Pi_{2^n} S_n K_n S_{n-1} K_{n-1} \dots S_{i+1} K_{i+1} S_i K_i \dots S_2 K_2 S_1 K_1 P_{2^n},$$

where  $n$  is an integer;  $F_{2^n}$  is a radix-2 FFT for a  $2^n$ -dimensional vector;  $\Pi_{2^n}$ ,  $S_i$  (where  $i$  is an integer), and  $P_{2^n}$  are various permutation operators or matrices; and the  $K_i$  are arithmetic operators.

Figure 2 depicts the proposed architecture. The permutation operators would be implemented by QCA modules, while the arithmetic operators  $K_i$  would be implemented by VLSI modules containing simple bit-serial processing elements. Each processing element would receive input data from two sources and would produce two outputs by performing simple multiplication and addition operations. Aside from being driven by the same clock (in order to obtain the necessary global synchronization), the processing elements would operate independently of each other; because of this feature, the processing modules would be amenable to large-scale implementation in complementary metal oxide/semiconductor (CMOS) VLSI circuitry. To obtain the necessary global synchronization, the VLSI and the QCA modules would be driven by the same clock.

*This work was done by Amir Fijany, Nikzad Toomarian, Katayoon Modarres, and Matthew Spotnitz of Caltech for NASA's Jet Propulsion Laboratory. Further information is contained in a TSP (see page 1). NPO-20923*

## Arrays of Carbon Nanotubes as RF Filters in Waveguides

Advantages would include compactness and high Q.

NASA's Jet Propulsion Laboratory, Pasadena, California

Brushlike arrays of carbon nanotubes embedded in microstrip waveguides provide highly efficient (high-Q) mechanical resonators that will enable ultra-miniature radio-frequency (RF) integrated circuits. In its basic form, this invention is an RF filter based on a carbon nanotube array embedded in a microstrip (or coplanar) waveguide, as shown in Figure 1. In addition, arrays of these nanotube-based RF filters can be used as an RF filter bank.

Applications of this new nanotube array device include a variety of communications and signal-processing technologies. High-Q resonators are essential for stable, low-noise communications, and radar ap-

plications. Mechanical oscillators can exhibit orders of magnitude higher Qs than electronic resonant circuits, which are limited by resistive losses. This has motivated the development of a variety of mechanical resonators, including bulk acoustic wave (BAW) resonators, surface acoustic wave (SAW) resonators, and Si and SiC micromachined resonators (known as "microelectromechanical systems" or MEMS). There is also a strong push to extend the resonant frequencies of these oscillators into the GHz regime of state-of-the-art electronics. Unfortunately, the BAW and

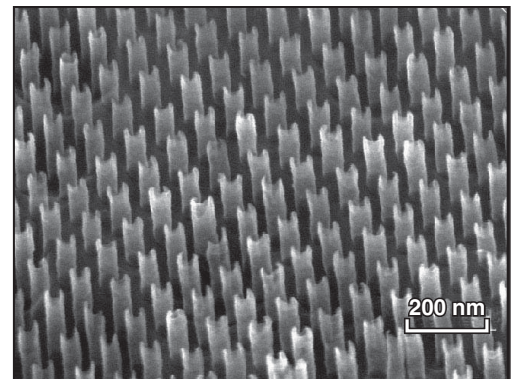


Figure 1. This Array of Carbon Nanotubes, with a diameter nonuniformity of <5 percent, was fabricated in a process that included the use of a nanopore template (J. Xu et al.).

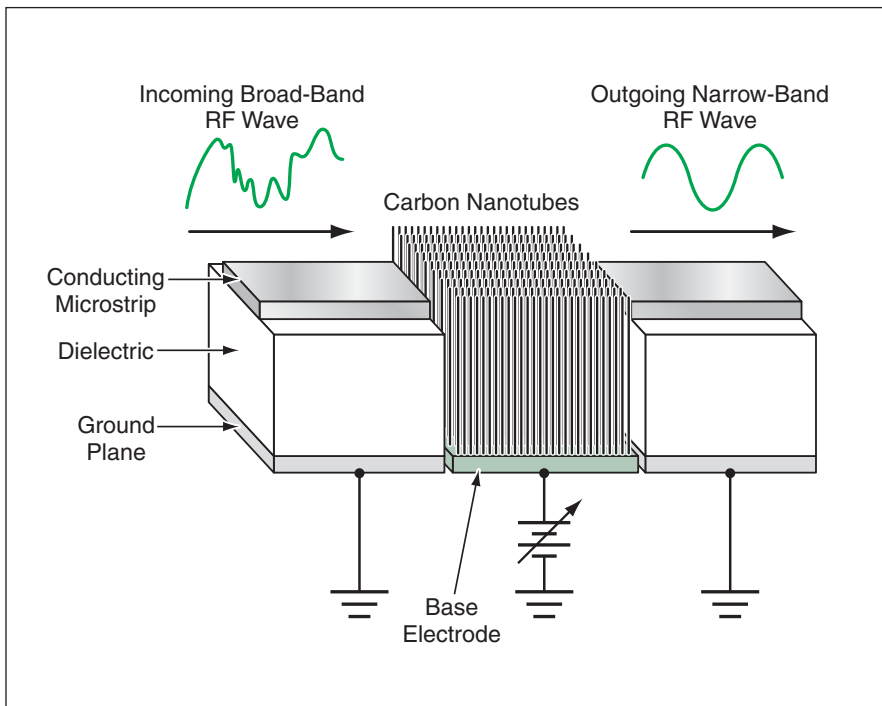


Figure 2. A Brushlike Array of Carbon Nanotubes embedded in a microstrip waveguide would act as a band-pass filter.

SAW devices tend to be large and are not easily integrated into electronic circuits. MEMS structures have been integrated into circuits, but efforts to extend MEMS resonant frequencies into the GHz regime have been difficult because of scaling problems with the capacitively-coupled drive and readout. In contrast, the proposed devices would be much smaller and hence could be more readily incorporated into advanced RF (more specifically, microwave) integrated circuits.

During the past few years, techniques for fabricating highly-ordered, dense arrays of nearly uniform carbon-nanotube cantilevers like so many bristles of a

brush (see Figure 1) have provided the essential basis for this new device. The basic principle of operation of such an array as band-pass filter is excitation of a mechanical (acoustic) deformation of the nanotubes by an incident RF wave (Figure 2). Coupling between the RF signal and the nanotubes is provided by Coulomb forces on electric charges in the nanotubes. The device functions as a narrow-band RF filter because incident waves are reflected from the metallic nanotubes, except at the mechanical resonant frequency of the array. The high-Q mechanical resonance of the uniform nanotube array filters the incoming RF signal and couples the RF

wave at the resonance frequency into the output electrode.

The resonance frequency of a nanotube cantilever depends on its diameter and length. For example, it is estimated that the resonance frequency of a carbon nanotube 10 nm in diameter and 100 nm long would be about 4 GHz. By adjusting the dimensions of the nanotubes in the array, it should be possible to select resonance frequencies that range from below 100 kHz up to tens of GHz.

There have also been attempts to make mechanical resonators using silicon cantilevers. However, the silicon devices investigated thus far have been limited to operation at frequencies below 400 MHz, whereas carbon-nanotube devices with Q values of the order of  $10^3$  at a frequency of 2 GHz have been demonstrated. Moreover, there are experimental data that suggest that carbon nanotube resonators should exhibit linear response over a larger dynamic range relative to silicon mechanical resonators.

*This work was done by Daniel Hoppe, Brian Hunt, Michael Hoenk, and Flavio Noca of Caltech for NASA's Jet Propulsion Laboratory and by Jimmy Xu of Brown University. Further information is contained in a TSP (see Page 1).*

*In accordance with Public Law 96-517, the contractor has elected to retain title to this invention. Inquiries concerning rights for its commercial use should be addressed to*

*Intellectual Property group*

*JPL*

*Mail Stop 202-233*

*4800 Oak Grove Drive*

*Pasadena, CA 91109*

*(818) 354-2240*

*Refer to NPO-30207, volume and number of this NASA Tech Briefs issue, and the page number.*

## Carbon Nanotubes as Resonators for RF Spectrum Analyzers

Compact, high-speed, high-Q spectrum analyzers could be integrated with other circuits.

NASA's Jet Propulsion Laboratory, Pasadena, California

Electromechanical resonators of a proposed type would comprise single carbon nanotubes suspended between electrodes (see Figure 1). Depending on the nanotube length, diameter, and tension, these devices will resonate at frequencies in a range from megahertz through gigahertz. Like the carbon-nanotube resonators described in the preceding article, these devices will exhibit high quality factors (Q

values), will be compatible with integration with electronic circuits, and, unlike similar devices made from silicone and silicone carbide, will have tunable resonant frequencies as high as several GHz.

An efficient electromechanical transduction method for the carbon nanotube resonators is provided by the previously observed variation of carbon nanotube length with charge injection. It was found

that injection of electrons or holes, respectively, lengthens or shortens carbon nanotubes, by amounts of the order of a percent at bias levels of a few volts. The charge-dependent length change also enables a simple and direct means of tuning the resonant frequency by varying the DC bias and hence the tension along the tube, much like tuning a guitar string.

In its basic form, the invention is a tun-

able high-Q resonator based on a suspended carbon nanotube bridge with attached electrodes (see Figure 1). An applied DC bias controls the tension and

thus the frequency of resonance. If one were to superimpose a radio-frequency (RF) bias on the DC bias, then the resulting rapid variation in tension or length

would set the tube into vibration. If, on the other hand, the carbon nanotube were to be set into vibration by interaction between an incident RF electric field and electric charges in the nanotube, then the vibration would give rise to an RF signal output that is proportional to the RF amplitude at the resonance frequency.

Because the transduction mechanism is extremely sensitive and the active volume is only a few nanometers in diameter, this device is not well suited for use as a microwave power device. Instead, this carbon nanotube mechanical resonator would be useful primarily as part of a highly precise, sensitive, frequency-selective detector. An array of such devices featuring nanotubes of different lengths (and thus different frequencies) could be made to operate as a high-speed spectrum analyzer (see Figure 2).

*This work was done by Brian Hunt, Flavio Noca, and Michael Hoenk of Caltech for NASA's Jet Propulsion Laboratory. Further information is contained in a TSP (see page 1).*

*In accordance with Public Law 96-517, the contractor has elected to retain title to this invention. Inquiries concerning rights for its commercial use should be addressed to*

*Intellectual Property group*

*JPL*

*Mail Stop 202-233*

*4800 Oak Grove Drive*

*Pasadena, CA 91109*

*(818) 354-2240*

*Refer to NPO-30206, volume and number of this NASA Tech Briefs issue, and the page number.*

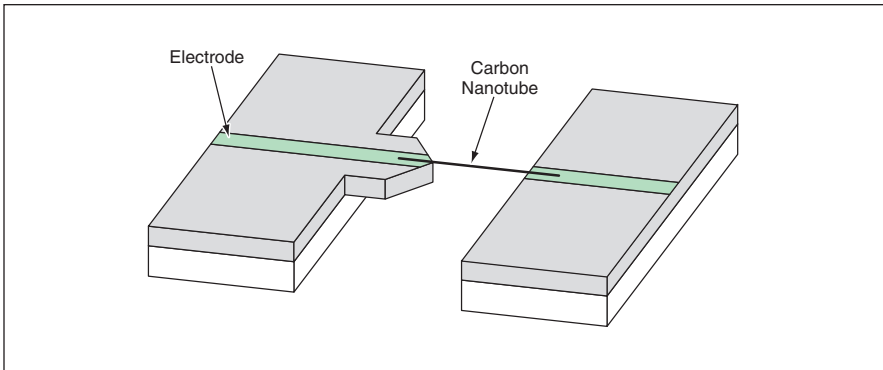


Figure 1. A **Carbon Nanotube Suspended Between Electrodes** could be stretched taut so that it would resonate in the same manner as that of a string on a musical instrument. It could serve as a tunable, high-Q resonator for a signal processor or a sensor.

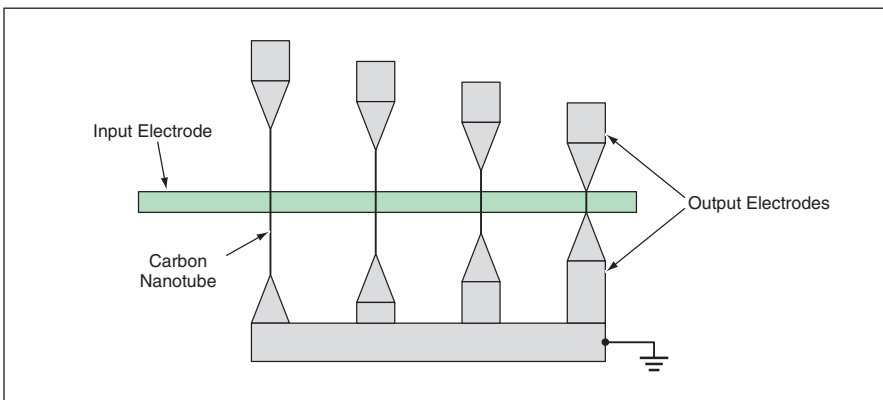


Figure 2. An **Array of Devices** like that of Figure 1, containing nanotubes of different lengths would be combined with an input electrode to construct an electromagnetic-spectrum analyzer that would function somewhat like a cochlea.





### Software for Viewing Landsat Mosaic Images

A Windows-based computer program has been written to enable novice users (especially educators and students) to view images of large areas of the Earth (e.g., the continental United States) generated from image data acquired in the Landsat observations performed circa the year 1990. The large-area images are constructed as mosaics from the original Landsat images, which were acquired in several wavelength bands and each of which spans an area (in effect, one tile of a mosaic) of  $\approx 5^\circ$  in latitude by  $\approx 6^\circ$  in longitude. Whereas the original Landsat data are registered on a universal transverse Mercator (UTM) grid, the program converts the UTM coordinates of a mouse pointer in the image to latitude and longitude, which are continuously updated and displayed as the pointer is moved. The mosaic image currently on display can be exported as a Windows bitmap file. Other images (e.g., of state boundaries or interstate highways) can be overlaid on Landsat mosaics. The program interacts with the user via standard toolbar, keyboard, and mouse user interfaces. The program is supplied on a compact disk along with tutorial and educational information.

*This program was written by Zack Watts, Catharine L. Farve, and Craig Harvey of PixSell, Inc., for Stennis Space Center.*

*In accordance with Public Law 96-517, the contractor has elected to retain title to this invention. Inquiries concerning rights for its commercial use should be addressed to*

*PixSell, Inc.*

*Building 2105*

*Stennis Space Center, MS 39529*

*Refer to SSC-00148, volume and number of this NASA Tech Briefs issue, and the page number.*

### Updated Integrated Mission Program

Integrated Mission Program (IMP) is a computer program for simulating spacecraft missions around the Earth, Moon, Mars, and/or other large bodies. IMP solves the differential equations of motion by use of a Runge-Kutta numerical-integration algorithm. Users control missions through selection from a large menu of events and maneuvers. Mission profiles,

time lines, propellant requirements, feasibility analyses, and perturbation analyses can be computed quickly and accurately. A prior version of IMP, written in FORTRAN 77, was reported in "Program Simulates Spacecraft Missions" (MFS-28606), *NASA Tech Briefs*, Vol. 17, No. 4 (April 1993), page 60. The present version, written in double-precision Lahey™ FORTRAN 90, incorporates a number of improvements over the prior version. Some of the improvements modernize the code to take advantage of today's greater central-processing-unit speeds. Other improvements render the code more modular; provide additional input, output, and debugging capabilities; and add to the variety of maneuvers, events, and means of propulsion that can be simulated. The IMP user manuals (of which there are now ten, each addressing a different aspect of the code and its use) have been updated accordingly.

*This program was written by Vincent A. Davuro, Sr., of Alpha Technology, Inc., for Marshall Space Flight Center. Further information is contained in a TSP (see page 1). MFS-31695*

### Software for Sharing and Management of Information

DIAMS is a set of computer programs that implements a system of collaborative agents that serve multiple, geographically distributed users communicating via the Internet. DIAMS provides a user interface as a Java applet that runs on each user's computer and that works within the context of the user's Internet-browser software. DIAMS helps all its users to manage, gain access to, share, and exchange information in databases that they maintain on their computers. One of the DIAMS agents is a personal agent that helps its owner find information most relevant to current needs. It provides software tools and utilities for users to manage their information repositories with dynamic organization and virtual views. Capabilities for generating flexible hierarchical displays are integrated with capabilities for indexed-query searching to support effective access to information. Automatic indexing methods are employed to support users' queries and communication between agents. The catalog of a repository is kept in object-oriented storage to facilitate sharing of information. Collaboration between

users is aided by matchmaker agents and by automated exchange of information. The matchmaker agents are designed to establish connections between users who have similar interests and expertise.

*This program was written by James R. Chen of Ames Research Center and Shawn R. Wolfe and Stephen D. Wragg of Caelum Research. Further information is contained in a TSP (see page 1). ARC-14654*

### Update on Integrated Optical Design Analyzer

Updated information on the Integrated Optical Design Analyzer (IODA) computer program has become available. IODA was described in "Software for Multidisciplinary Concurrent Optical Design" (MFS-31452), *NASA Tech Briefs*, Vol. 25, No. 10 (October 2001), page 8a. To recapitulate: IODA facilitates multidisciplinary concurrent engineering of highly precise optical instruments. The architecture of IODA was developed by reviewing design processes and software in an effort to automate design procedures. IODA significantly reduces design iteration cycle time and eliminates many potential sources of error. IODA integrates the modeling efforts of a team of experts in different disciplines (e.g., optics, structural analysis, and heat transfer) working at different locations and provides seamless fusion of data among thermal, structural, and optical models used to design an instrument. IODA is compatible with data files generated by the NASTRAN™ structural-analysis program and the Code V® optical-analysis program, and can be used to couple analyses performed by these two programs. IODA supports multiple-load-case analysis for quickly accomplishing trade studies. IODA can also model the transient response of an instrument under the influence of dynamic loads and disturbances.

*This program was written by James D. Moore, Jr., and Ed Troy of SRS Technologies for Marshall Space Flight Center. Further information is contained in a TSP (see page 1). MFS-31809*





## Optical-Quality Thin Polymer Membranes

Surface roughnesses and thickness variations are small enough for demanding scientific applications.

*Marshall Space Flight Center, Alabama*

A method of fabricating both curved and flat thin polymer membranes of optical quality has been developed. The method was originally intended to enable the fabrication of lightweight membrane imaging and interferometric optics, possibly with apertures multiple meters wide, for use in scientific instruments that would operate in outer space. The method may also be applicable to the fabrication of lightweight membrane optics for terrestrial use.

The method involves flow-casting of a soluble polymer with mechanical and

environmental controls that provide nearly ideal conditions for the formation of a membrane. The preferred environmental conditions and other details of the process depend on the choice of polymer and substrate material and on the shape and size of the membrane to be cast. Once the polymer has dried to a membrane, it is cured with convective heating, then released.

Membranes with root-mean-square surface roughnesses of  $<10.5 \text{ \AA}$  can be produced routinely by this method. Variations in the thicknesses of the mem-

branes have ranged from  $1/3$  wavelength down to as little as  $1/20$  wavelength (at a wavelength of 633 nm). Membranes fabricated thus far have had diameters up to 0.5 m, and there appears to be no major obstacle to scaling up to multiple-meter diameters.

*This work was done by James Moore and Brian Patrick for Marshall Space Flight Center. Further information is contained in a TSP (see Page 1).*

*MFS-31718*





## Rollable Thin Shell Composite-Material Paraboloidal Mirrors

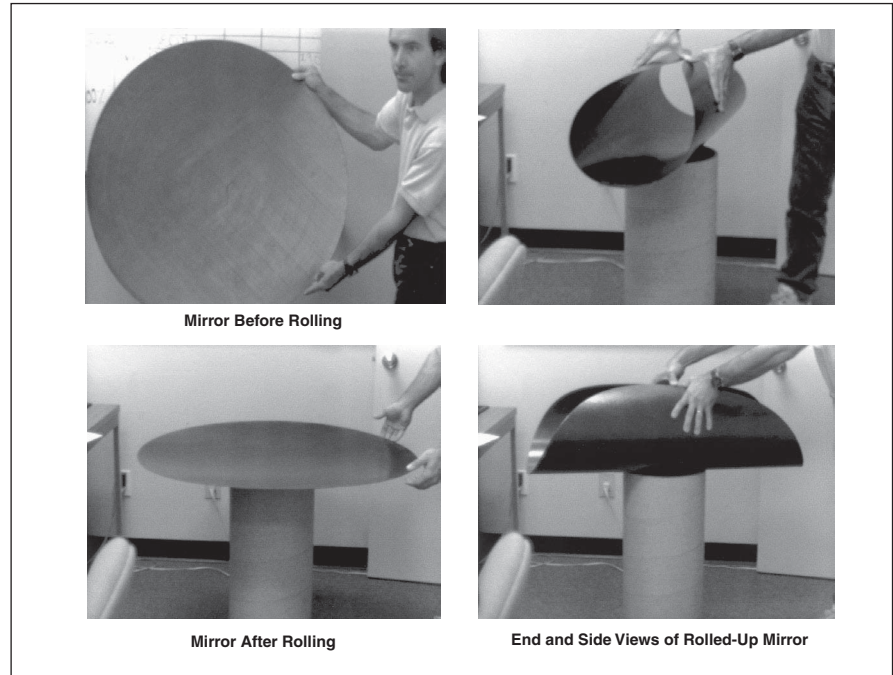
These lightweight focusing mirrors can be stored in fairly narrow cylinders.

NASA's Jet Propulsion Laboratory, Pasadena, California

An experiment and calculation have demonstrated the feasibility of a technique of compact storage of paraboloidal mirrors made of thin composite-material (multiple layers of carbon fiber mats in a polymeric matrix) shells coated with metal for reflectivity. Such mirrors are under consideration as simple, lightweight alternatives to the heavier, more complex mirrors now used in space telescopes. They could also be used on Earth in applications in which gravitational sag of the thin shells can be tolerated.

The present technique is essentially the same as that used to store large maps, posters, tapestries, and similar objects: One simply rolls up the mirror to a radius small enough to enable the insertion of the mirror in a protective cylindrical case. Provided that the stress associated with rolling the mirror is not so large as to introduce an appreciable amount of hysteresis, the mirror can be expected to spring back to its original shape, with sufficient precision to perform its intended optical function, when unrolled from storage.

A simple calculation yields a qualitative indication of the level of stress in, and the likelihood of permanent deformation of, a rolled mirror. The calculation in question is an estimate of the stress in a rolled flat sheet of the same composite material and thickness as those of the mirror shell. The compressive or tensile stress ( $S$ ) in the radially innermost or radially outermost surface layer, respectively, is given by  $S = Et/2r$ , where  $E$  is the modulus of elasticity of the composite-material shell or flat sheet,  $t$  is the thickness of the shell or flat sheet, and  $r$  is the radius of curvature



A Thin-Shell Composite-Material Mirror was rolled, then unrolled without introducing visible permanent distortion of its optical surface.

to which the shell or sheet is rolled. For a typical mirror diameter ( $D = 2$  m) and shell thickness ( $t = 1$  mm) rolled to a radius such that diametrically opposite points on the edge of the mirror just come into contact ( $r = D/2\pi$ ), this equation yields  $S \approx 0.016E$ . This is a relatively small amount of stress and, as such, would not be expected to cause an appreciable permanent deformation.

The figure depicts stages of a demonstration in which a composite-material

mirror of  $D = 90$  cm,  $t = 1$  mm, and a focal ratio ( $f$  number) of 1 was manually rolled as described above. Visual inspection after unrolling revealed no hysteresis. Further optical testing of the unrolled mirror was underway at the time of reporting the information for this article.

*This work was done by Aden Meinel, Marjorie Meinel, and Robert Romeo of Caltech for NASA's Jet Propulsion Laboratory. Further information is contained in a TSP (see page 1). NPO-20987*

## Folded Resonant Horns for Power Ultrasonic Applications

Ultrasonic actuators can be made shorter.

NASA's Jet Propulsion Laboratory, Pasadena, California

Folded horns have been conceived as alternatives to straight horns used as resonators and strain amplifiers in power ultrasonic systems. Such systems are used for cleaning, welding, solder-

ing, cutting, and drilling in a variety of industries. In addition, several previous *NASA Tech Briefs* articles have described instrumented drilling, coring, and burrowing machines that utilize

combinations of sonic and ultrasonic vibrational actuation. The main advantage of a folded horn, relative to a straight horn of the same resonance frequency, is that the folded horn can

be made shorter (that is, its greatest linear dimension measured from the outside can be made smaller). Alternatively, for a given length, the resonance frequency can be reduced. Hence, the folded-horn concept affords an additional degree of design freedom for reducing the length of an ultrasonic power system that includes a horn.

Figure 1 depicts an ultrasonic actuator that includes a straight stepped horn, one that includes an inverted

straight stepped horn of approximately the same resonance frequency, and one that includes a folded stepped horn of approximately the same resonance frequency. The main role of the straight stepped horn is to amplify longitudinal strain at its outermost end. In the folded version, one can exploit bending strain in addition to longitudinal strain, and by adjusting the thickness of the folds, one can increase or decrease the contributions of bending displacements

to the overall displacement at the tip. In this case, the folded-horn concept not only yields a shorter horn, but by enabling utilization of bending displacements, it also affords an additional degree of design freedom. Figure 2 shows an experimental folded-horn actuator of 16-kHz resonance frequency alongside a straight-horn actuator of 20-kHz resonance frequency.

*This work was done by Stewart Sherrit, Stephen Askins, Michael Gradziel, Xiaoqi Bao, Zensheu Chang, Benjamin Dolgin, and Yoseph Bar-Cohen of Caltech and Tom Peterson of Cybersonics Inc. for NASA's Jet Propulsion Laboratory. Further information is contained in a TSP (see page 1). NPO-30489*

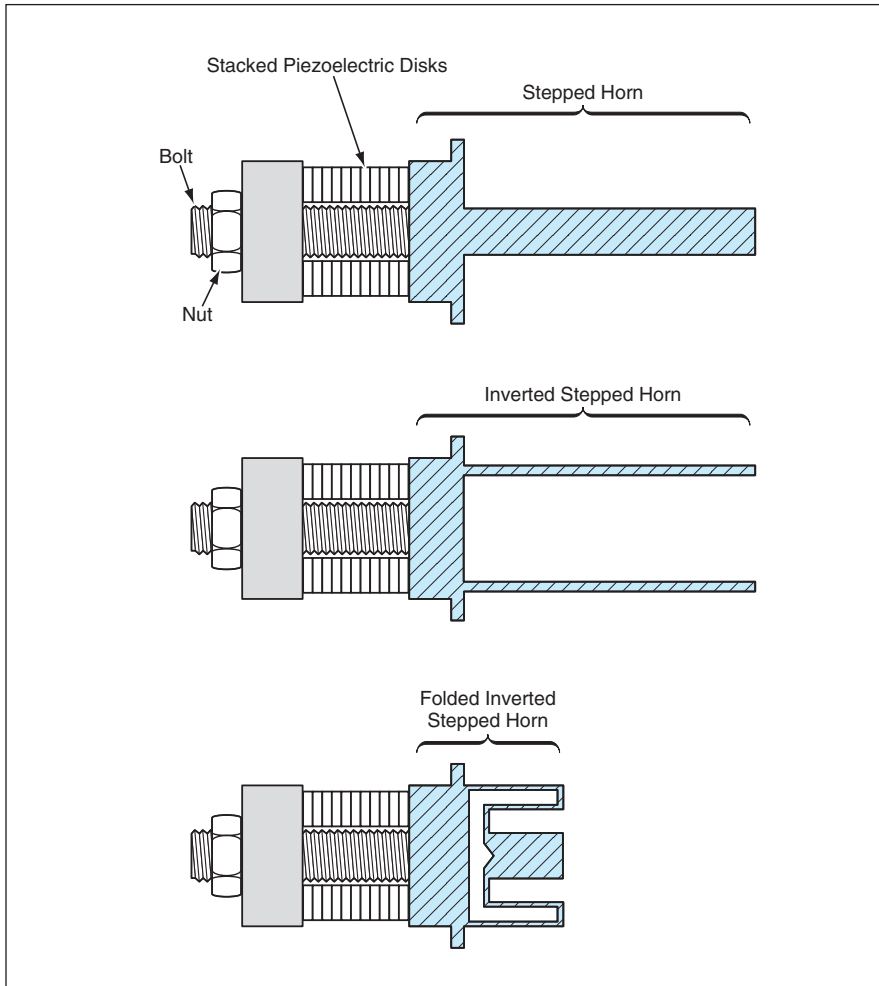


Figure 1. Three Similar Power Ultrasonic Actuators are depicted partly in cross sections to illustrate a progression of designs from a straight stepped horn to a folded inverted stepped horn.

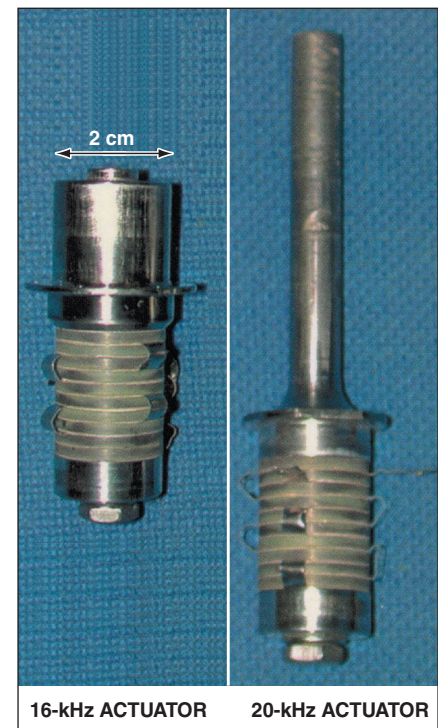


Figure 2. The Overall Length of the 16-kHz Horn is Shorter than the 20-kHz horn by virtue of being folded. The distance the acoustic wave travels has been designed to be the same. The lower frequency in the folded horn is due to reduced clamping and bending at the folds.

## Touchdown Ball-Bearing System for Magnetic Bearings

In the event of a touchdown, ball bearings provide full support.

*John H. Glenn Research Center, Cleveland, Ohio*

The torque-limited touchdown bearing system (TLTBS) is a backup mechanical-bearing system for a high-speed rotary machine in which the rotor shaft is supported by magnetic bearings in steady-state normal operation. The TLTBS provides ball-bearing support to augment or supplant the magnetic bearings during startup, shutdown, or failure of the magnetic bearings. The TLTBS also provides support in the presence of conditions (in particular, rotational acceleration) that make it difficult or impossible to control the magnetic bearings or in which the magnetic bearings are not strong enough (e.g., when the side load against the rotor exceeds the available lateral magnetic force).

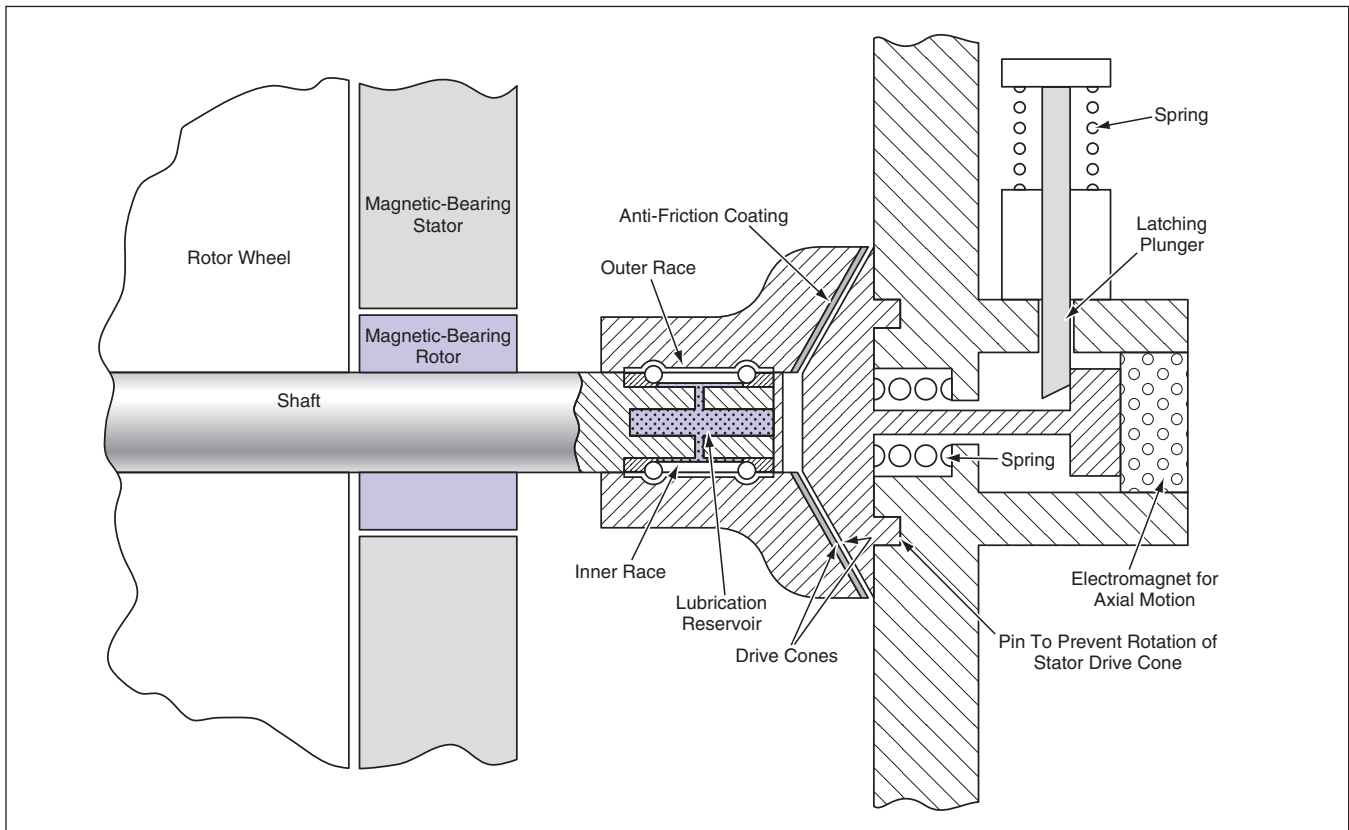
The TLTBS includes two similar or identical subsystems, each located at one end of the rotor shaft (see figure). Mounted inside each female cone is a specially designed high-speed bearing with a built-in

lubrication system. Mounted on the stator is (1) a non-rotating drive cone capable of mating with the drive cone on the rotor and (2) an electromagnetically actuated inserter mechanism that moves the stator drive cone axially between two extreme positions as described in more detail in the next paragraph. The inserter mechanism contains two electromagnets: one that withdraws the spring-loaded plunger, the second to withdraw the latch when insertion is required. Electric power is applied to the inserter mechanism only during the fraction of a second needed for the axial motion: no power is needed to keep the stator drive cone latched at either extreme position.

In one extreme axial position, denoted the inserted position, the stator drive cone is in contact with the outer-bearing-race drive cone under spring load. In this position, the ball-bearing assembly carries the full bearing load.

The other extreme axial position (the one shown in the figure) is denoted the retracted position. In this position, the stator drive cone is withdrawn from the rotor drive cone to an axial clearance of 0.010 in. ( $\approx 0.25$  mm). During normal operation in the retracted position, the shaft is fully supported by the magnetic bearing. The clearance between drive cones is small enough that if the magnetic bearing fails or if an excessive side load occurs, the ball-bearing assembly can provide full support, preventing damage to the magnetic suspension and making it possible to continue (at least temporarily) operation of the machine.

Because the stator drive cone does not rotate and the rotor drive cone rotates at high speed during normal operation of the magnetic bearing, it is necessary to accommodate, and prevent frictional damage by, the slip that occurs between the two drive



The Portion of the TLTBS at One End of a Rotor Shaft includes a ball-bearing assembly and drive cones that can be either mated or separated by a small clearance as shown here.

cones at the time of initial contact. For this purpose, the mating surfaces of the drive cones are coated with dry lubricant films. In addition, the ball-bearing assembly contains a reservoir designed to dispense lubricant to support an elastohydrodynamic film for the specified lifetime of the system.

*This work was done by Edward P. Kingsbury, Robert Price, Erik Gelotte, and Herbert B. Singer of The Bearing Consultants, LLP for Glenn Research Center. Further information is contained in a TSP (see page 1).*

*Inquiries concerning rights for the commercial use of this invention should be ad-*

*ressed to NASA Glenn Research Center, Commercial Technology Office, Attn: Steve Fedor, Mail Stop 4-8, 21000 Brookpark Road, Cleveland, Ohio 44135. Refer to LEW-17282.*

## ❁ Flux-Based Deadbeat Control of Induction-Motor Torque

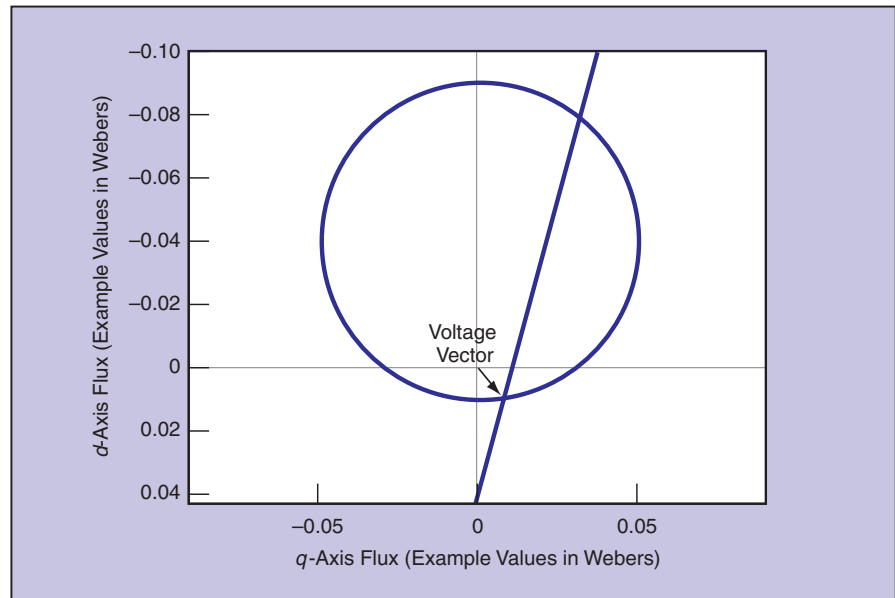
Graphical constructions provide insight into solutions of control problems.

John H. Glenn Research Center, Cleveland, Ohio

An improved method and prior methods of deadbeat direct torque control involve the use of pulse-width modulation (PWM) of applied voltages. The prior methods are based on the use of stator flux and stator current as state variables, leading to mathematical solutions of control equations in forms that do not lend themselves to clear visualization of solution spaces. In contrast, the use of rotor and stator fluxes as the state variables in the present improved method lends itself to graphical representations that aid in understanding possible solutions under various operating conditions. In addition, the present improved method incorporates the superposition of high-frequency carrier signals for use in a motor-self-sensing technique for estimating the rotor shaft angle at any speed (including low or even zero speed) without need for additional shaft-angle-measuring sensors.

Prerequisite to a description of the method is a description of the concept of  $dq$  variables and  $dq$  coordinates. The “ $d$ ” and “ $q$ ” signify “direct” and “quadrature,” respectively. The  $dq$  coordinates lie along two orthogonal axes attached to the stator. The  $dq$  coordinates and the  $dq$  variables (which can be, for example, phase voltages and fluxes projected onto the  $dq$  coordinates) are commonly used in the design and analysis of induction motors.

The derivation of the method begins with the observation that a desired change in the torque of an induction motor can be represented as a straight line with units of flux on both axes of the  $d-q$  plane. The equation that describes the straight line can be derived from the discrete form of the induction-motor equations by use of the stator and rotor fluxes as state variables. The desired change in stator flux can be represented as a circle on the  $d-q$  plane. The voltage needed to achieve the desired change in torque and change in stator flux



A Straight Line and a Circle in the  $d-q$  Plane represent the desired change in torque and the desired change in stator flux, respectively. The voltage vector needed to achieve the desired change in torque and change in stator flux in one time step can be found from one of the intersections of line and the circle.

in one time step can be found from an intersection of the torque line and stator-flux circle (see figure).

Going beyond the aforementioned graphical representations, the maximum-current operating limits can be represented as a set of two lines parallel to the torque line. The maximum-voltage operating limits can be represented as a hexagon on the  $d-q$  plane. The maximum-voltage hexagon can be divided into four regions corresponding to an increase or decrease in torque and an increase or decrease in flux. As a result, the effect of a particular voltage vector (increase or decrease in torque or flux) can be clearly seen.

A control algorithm based on the graphical constructions and the underlying equations has been developed. The algorithm causes the synthesis of the needed excitation voltages by use of space vector modulation techniques to calculate and command inverter duty cy-

cles. In the implementation of the algorithm without shaft-angle-measuring sensors, the high-frequency voltage needed for sensorless operation is added to the fundamental voltage and used as input for the PWM calculations. The PWM portion of the control algorithm then determines the duty cycles to generate both voltages at once. The signal from the resulting high-frequency current is processed to estimate the angular position and speed of the rotor.

*This work was done by Barbara H. Kenny of Glenn Research Center and Robert D. Lorenz of the University of Wisconsin. Further information is contained in a TSP (see page 1).*

*Inquiries concerning rights for the commercial use of this invention should be addressed to NASA Glenn Research Center, Commercial Technology Office, Attn: Steve Fedor, Mail Stop 4-8, 21000 Brookpark Road, Cleveland, Ohio 44135. Refer to LEW-17329.*



## Block Copolymers as Templates for Arrays of Carbon Nanotubes

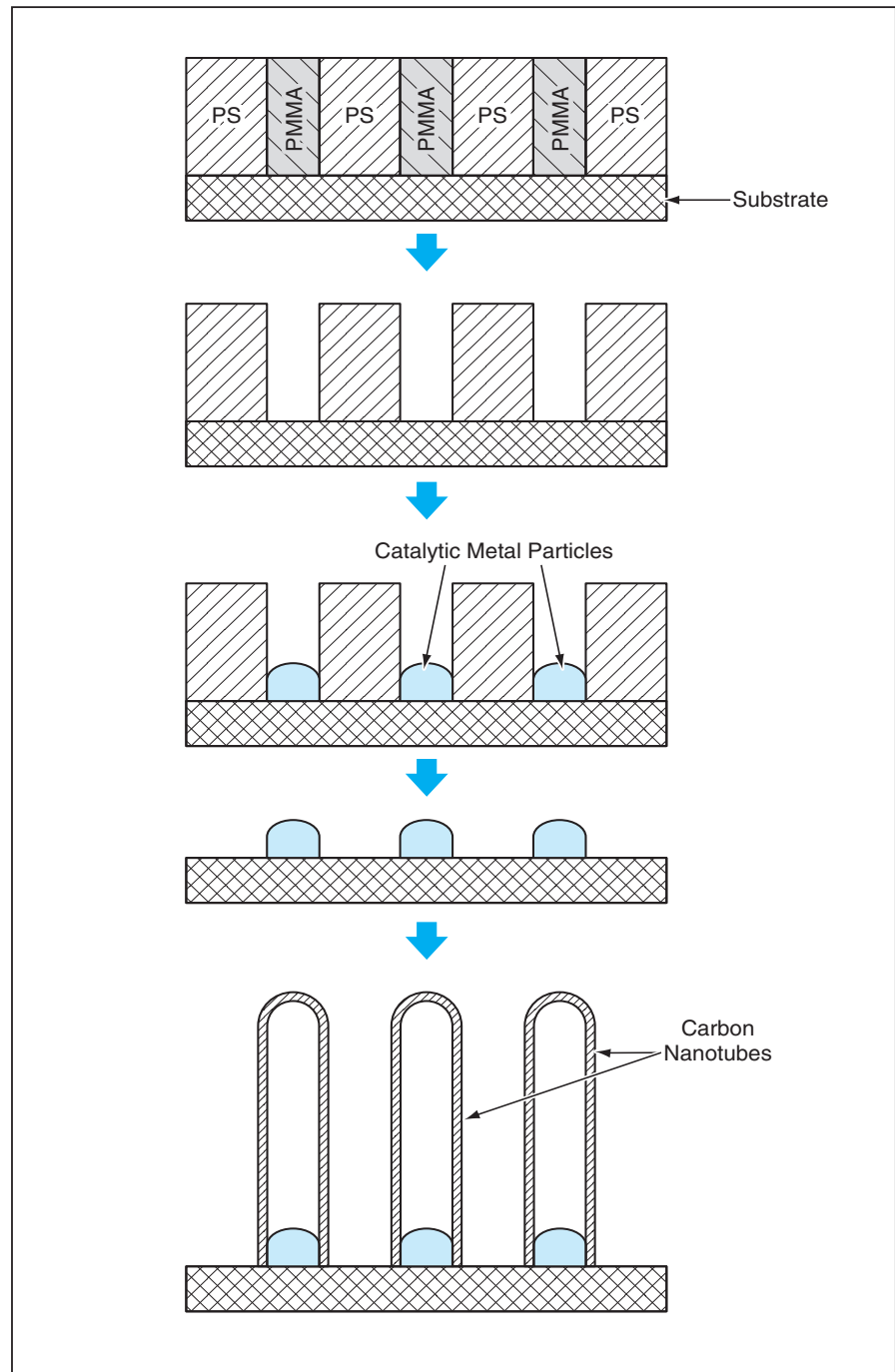
The spontaneous formation of nanostructures in block copolymers would be exploited.

*NASA's Jet Propulsion Laboratory, Pasadena, California*

A method of manufacturing regular arrays of precisely sized, shaped, positioned, and oriented carbon nanotubes has been proposed. Arrays of carbon nanotubes could prove useful in such diverse applications as communications (especially for filtering of signals), biotechnology (for sequencing of DNA and separation of chemicals), and micro- and nanoelectronics (as field emitters and as signal transducers and processors). The method is expected to be suitable for implementation in standard semiconductor-device fabrication facilities.

As in previously reported methods, carbon nanotubes would be formed in the proposed method by decomposition of carbon-containing gases over nanometer-sized catalytic metal particles that had been deposited on suitable substrates. Unlike in previously reported methods, the catalytic metal particles would not be so randomly and densely distributed as to give rise to thick, irregular mats of nanotubes with a variety of lengths, diameters, and orientations. Instead, in order to obtain regular arrays of spaced-apart carbon nanotubes as nearly identical as possible, the catalytic metal particles would be formed in predetermined regular patterns with precise spacings. The regularity of the arrays would be ensured by the use of nanostructured templates made of block copolymers.

A block copolymer consists of two or more sections, or "blocks," each of which consists of a controlled number of monomers of a given type. Some combinations of monomers (for example, styrene and methylmethacrylate or styrene and butadiene) yield block copolymer molecules that, under appropriate conditions (for example, when heated above their glass-transition temperatures for 10 to 20 hours) assemble themselves into repeating structures with unit-cell dimensions that typically range between 5 and 100 nm. In other words, a block copolymer can be made to acquire a regular structure on a length scale substantially larger than the individual monomer units



A Template for Deposition of catalytic metal particles would be formed in a PS/PMMA block copolymer, then carbon nanotubes would be grown on the particles by decomposition of carbon-containing gas molecules.

yet well below a macroscopic scale. For example, when heated in an electric field, a thin film of molecules of a block copolymer consisting of sections of polystyrene (PS) connected to sections of poly(methylmethacrylate) [PMMA] undergoes a nanoscale phase separation, forming aligned, regularly-spaced cylinders of PMMA spaced apart in a matrix of PS. The size and separation of the cylinders depends on the sizes of the PS and PMMA blocks in the molecules.

Proposed techniques for utilizing such nanostructured block copolymers as templates are generally oriented toward exploiting the differences between chemical and/or physical properties of the different materials in the adjacent nanoscale regions. In particular, one could utilize differences in reactivities of the blocks with respect to one or more chemical(s) in order to selectively remove the blocks of one type, without removing the adjacent blocks of the other

type, in order to create voids into which catalytic metals could be deposited.

In a typical application (see figure), one would begin by coating a substrate with a film of PS/PMMA diblock copolymer. (A typical substrate material would be silicon with a surface layer of silicon oxide.) The block copolymer film would be treated to form the desired repeating nanostructure. The nanostructured block copolymer would be exposed to ultraviolet light or to high-energy electrons, either of which would degrade the PMMA more than it would degrade the PS. The workpiece would be washed in acetic acid to remove the degraded PMMA, yielding a substrate covered with a thin film of polystyrene containing a regular array of nanometer-sized holes, into which catalytic metal could be deposited either electrochemically or from vapor. The polystyrene would be removed from around the deposited metal particles by oxidation, solvation, or etch-

ing with reactive ions. Remaining on the substrate would be a regular array of catalytic metal dots, on which a regular array of carbon nanotubes could then be grown.

*This work was done by Michael Bronikowski and Brian Hunt of Caltech for NASA's Jet Propulsion Laboratory. Further information is contained in a TSP (see page 1).*

*In accordance with Public Law 96-517, the contractor has elected to retain title to this invention. Inquiries concerning rights for its commercial use should be addressed to*

*Intellectual Property group*

*JPL*

*Mail Stop 202-233*

*4800 Oak Grove Drive*

*Pasadena, CA 91109*

*(818) 354-2240*

*Refer to NPO-30240, volume and number of this NASA Tech Briefs issue, and the page number.*



## Throttling Cryogen Boiloff To Control Cryostat Temperature

Consumption of liquid cryogen and electrical energy could be reduced.

NASA's Jet Propulsion Laboratory, Pasadena, California

An improved design has been proposed for a cryostat of a type that maintains a desired low temperature mainly through boiloff of a liquid cryogen (e.g., liquid nitrogen) at atmospheric pressure. (A cryostat that maintains a low temperature mainly through boiloff of a cryogen at atmospheric pressure is said to be of the pour/fill Dewar-flask type because its main component is a Dewar flask, the top of which is kept open to the atmosphere so that the liquid cryogen can boil at atmospheric pressure and cryogenic liquid can be added by simply pouring it in.) The major distinguishing feature of the proposed design is control of temperature and cooling rate through control of the flow of cryogen vapor from a heat exchanger. At a cost of a modest increase in complexity, a cryostat according to the proposal would retain most of the compactness of prior, simpler pour/fill Dewar-flask cryostats, but would utilize cryogen more efficiently (intervals between cryogen refills could be longer).

In a typical prior variable-temperature cryostat of the pour/fill Dewar-flask type, a specimen (typically, an infrared photodetector) to be tested at a specified low temperature is mounted, along with a small electric heater, on a variable-temperature stage on one side of a thermal-resistance block. The other side of the thermal-resistance block is in contact with the cold inner wall of the cryogen reservoir (see figure). If it is desired to test the specimen at a temperature above the boiling temperature of the cryogen, then a proportional amount of power is supplied to the electric heater. Of course, the heat that leaks through the thermal-resistance block into the cryogen reservoir causes the cryogen to boil off faster than it otherwise would.

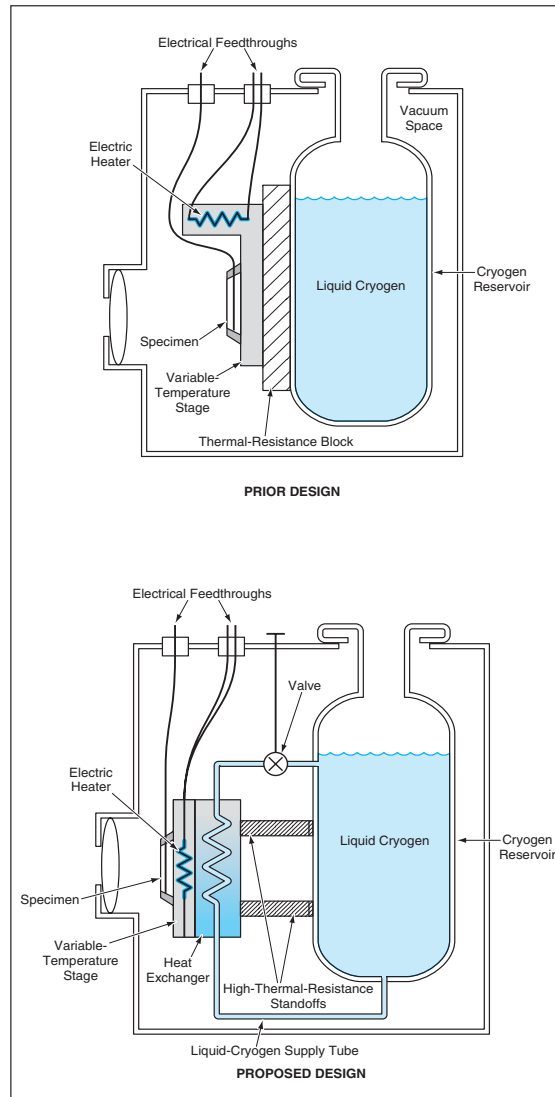
In the proposed cryostat, the variable-temperature stage holding the specimen and electric heater would be mounted on one surface of a heat exchanger that would be held away from

the cryogen reservoir by high-thermal-resistance standoffs. A tube would supply liquid cryogen from the bottom of

the cryogen reservoir, upward into the heat exchanger, by gravity feed. From the top of the heat-exchanger, boiled-off cryogen vapor would travel through a

tube and a valve, returning to the top of the reservoir. By using the valve to throttle the flow of vapor from the heat exchanger, one would control the flow of liquid to the heat exchanger, thereby controlling the rate of cooling and the temperature of the specimen. In addition, as before, one could raise the temperature of the specimen by use of the electric heater. To the extent to which one could maintain the desired temperature by flow control rather than electric heating, one could reduce the consumption of both liquid cryogen and electrical energy.

*This work was done by Thomas Cunningham of Caltech for NASA's Jet Propulsion Laboratory. Further information is contained in a TSP (see page 1). NPO-21186*



These **Variable-Temperature Cryostats** of the pour/fill-Dewar-flask type differ in the nature of the thermal resistance between the cryogen reservoir and the variable-temperature stage. The fixed thermal resistance of the prior design would be replaced, in the proposed design, by a variable thermal resistance implemented by use of a heat exchanger with a flow-control valve.



## Collaborative Software Development Approach Used To Deliver the New Shuttle Telemetry Ground Station

This software affords enhanced capabilities for utilizing telemetric data.

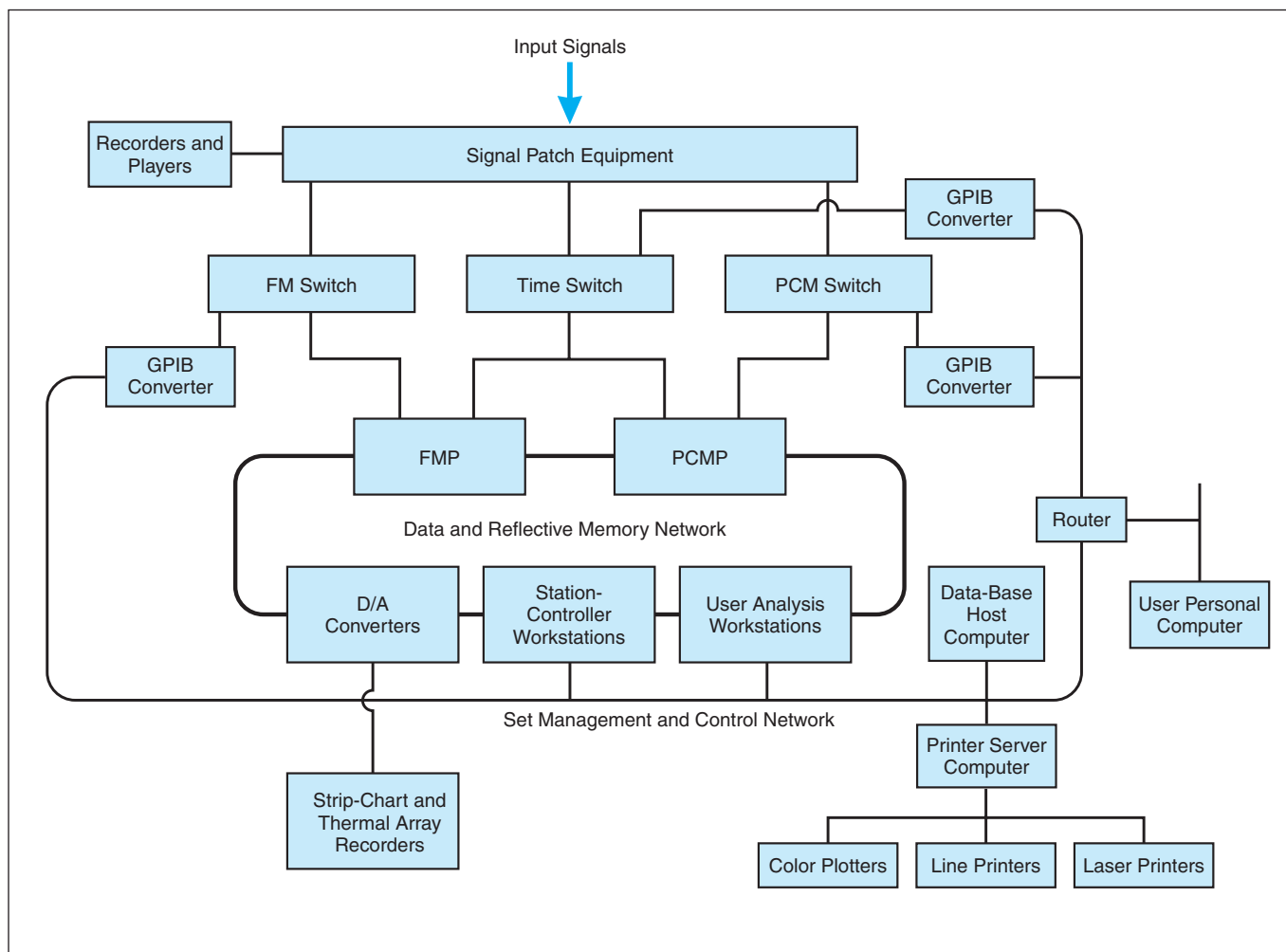
*John F. Kennedy Space Center, Florida*

United Space Alliance (USA) developed and used a new software development method to meet technical, schedule, and budget challenges faced during the development and delivery of the new Shuttle Telemetry Ground Station at Kennedy Space Center. This method, called Collaborative Software Development, enabled KSC to effectively leverage industrial software and build additional capabilities to meet shuttle system and operational requirements. Application of this method resulted in reduced time to market, reduced development cost, improved product quality, and improved

programmer competence while developing technologies of benefit to a small company in California (AP Labs Inc.). Many modifications were made to the baseline software product (VMEwindow), which improved its quality and functionality. In addition, six new software capabilities were developed, which are the subject of this article and add useful functionality to the VMEwindow environment. These new software programs are written in C or VX-Works and are used in conjunction with other ground station software packages, such as VMEwindow, Matlab, Dataviews, and PVWave.

The Space Shuttle Telemetry Ground Station receives frequency-modulation (FM) and pulse-code-modulated (PCM) signals from the shuttle and support equipment. The hardware architecture (see figure) includes Sun workstations connected to multiple PCM- and FM-processing VersaModule Eurocard (VME) chassis. A reflective memory network transports raw data from PCM Processors (PCMPs) to the programmable digital-to-analog (D/A) converters, strip chart recorders, and analysis and controller workstations.

The first new program provides VMEwindow access to the reflective



The Upgraded RPS includes, notably, a reflective memory network that serves as the primary means of transport of raw data.

memory via a Sun Sbus interface. This program makes it possible to acquire and display data from multiple real-time telemetry processors, with deterministic, minimal latency, at any of the ground-station Sun workstations.

Another program prompts the user to enter a mission number, parameters and measurement names for a specific PCM telemetry stream. The program then queries an Oracle database and creates a flat file with the appropriate information for setup of VME chassis. This file is then automatically imported to the setup configuration in VMEwindow. Prior to this development, the user was required to enter all stream parameters via a keyboard. This was an extremely time-consuming and laborious process, which was very prone to error. The program also retrieves and loads data to automatically generate trigger parameters, derived parameters, and mathematical formulas needed to process the retrieved data.

The third program affords capabilities for setting up and controlling a general-purpose interface bus (GPIB) circuit board to perform special FM-signal-processing functions. These functions include snapshots that provide average, minimum, and maximum values of 100

samples of data, and calibrations that provide an average of 5 samples at each of the 0-, 25-, 50-, 75-, and 100-percent data levels. The setup enables individual control of the discriminator and the switch, along with automated control of snapshots and calibrations. The setup functions of this program are integrated into the VMEwindow telemetry-control software and are accessible via an icon in a VMEwindow display. The control functions of this program are exerted via the driver software of the GPIB circuit board.

The fourth program provides for the setup and control of a digital-to-analog converter. As in the case of the third program, the setup functions of this program are integrated into the VMEwindow telemetry-control software and are accessible via an icon in a VMEwindow display. Control is provided by a driver subprogram that interprets the setup and controls the board accordingly to make it generate the required output.

The fifth program provides the ability to reconstitute major frames of data from single minor frame PCM data output from the PCMP decom. Shipping minor frames of data was required to provide minimum data latency and loss to the strip chart recorders in the event of a loss of the

telemetry signal. Major frames of minor frame data are fed to VMEwindow engineering conversion icons in order to take advantage of the displays and processing capabilities of VMEwindow.

The final software innovation "thus far" provides the capability to record selected parameters in real time and output this data to a formatted text file. This file can be viewed displaying near-time history of parameter values with associated time tags. The data can be displayed in decimal, hexadecimal, octal, binary, and engineering converted formats and either all data or change data can be stored.

The baseline ground station development effort spawned the first four of these innovations discussed. The last two discussed were developed under a continuing collaborative relationship between USA and AP Labs Inc., designed to improve shuttle processing and foster continued technological innovation.

*This work was done by Randy L. Kirby, David Mann, Stephen G. Prenger, Wayne Craig, Andrew Greenwood, Jonathan Morris, and Charles H. Fricker of United Space Alliance and Son Quach and Paul Lechese of AP Labs for **Kennedy Space Center**. Further information is contained in a TSP (see page 1).*

*KSC-12100/01/02/03/71/81*



### **Turbulence in Supercritical $O_2/H_2$ and $C_7H_{16}/N_2$ Mixing Layers**

This report presents a study of numerical simulations of mixing layers developing between opposing flows of paired fluids under supercritical conditions, the purpose of the study being to elucidate chemical-species-specific aspects of turbulence. The simulations were performed for two different fluid pairs —  $O_2/H_2$  and  $C_7H_{16}/N_2$  — at similar reduced initial pressures (reduced pressure is defined as pressure  $\div$  critical pressure). Thermodynamically,  $O_2/H_2$  behaves more nearly like an ideal mixture and has greater solubility, relative to  $C_7H_{16}/N_2$ , which departs strongly from ideality. Because of a specified smaller initial density stratification, the  $C_7H_{16}/N_2$  layers exhibited greater levels of growth, global molecular mixing, and turbulence. However, smaller density gradients at the transitional state for the  $O_2/H_2$  system were interpreted as indicating that locally, this system exhibits enhanced mixing as a consequence of its greater solubility and closer approach to ideality. These thermodynamic features were shown to affect entropy dissipation, which was found to be larger for  $O_2/H_2$  and concentrated in high-density-gradient-magnitude regions that are distortions of the initial density-stratification boundary. In  $C_7H_{16}/N_2$ , the regions of largest dissipation were found to lie in high-density-gradient-magnitude regions that result from mixing of the two fluids.

*This work was done by Josette Bellan, Kenneth Harstad, and Nora Okong'o of Caltech for NASA's Jet Propulsion Laboratory. Further information is contained in a TSP (see page 1).*  
NPO-30561

### **Time-Resolved Measurements in Optoelectronic Microbioanalysis**

A report presents discussion of time-resolved measurements in optoelectronic microbioanalysis. Proposed microbioanalytical “laboratory-on-a-chip” devices for detection of microbes and toxic chemicals would include optoelectronic sensors and associated electronic circuits that would look for fluorescence or phosphorescence signatures of multiple hazardous biomolecules in order to detect which ones were present in a given situation. The emphasis in the instant report is on gating an active-pixel sensor in the time domain, instead of filtering light in the wavelength domain, to prevent the sensor from responding to a laser pulse used to excite fluorescence or phosphorescence while enabling the sensor to respond to the decaying fluorescence or phosphorescence signal that follows the laser pulse. The active-pixel sensor would be turned on after the laser pulse and would be used to either integrate the fluorescence or phosphorescence signal over several lifetimes and many excitation pulses or else take time-resolved measurements of the fluorescence or phosphorescence. The report also discusses issues of multiplexing and of using time-resolved measurements of fluorophores with known different fluorescence lifetimes to distinguish among them.

*This work was done by Gregory Bearman and Dmitri Kossakovski of Caltech for NASA's Jet Propulsion Laboratory. Further information is contained in a TSP (see page 1).*

*In accordance with Public Law 96-517, the contractor has elected to retain title to this invention. Inquiries concerning rights for its commercial use should be addressed to*

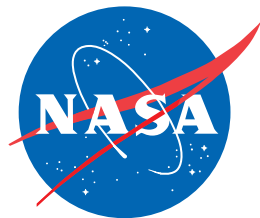
*Intellectual Property group  
JPL  
Mail Stop 202-233  
4800 Oak Grove Drive  
Pasadena, CA 91109  
(818) 354-2240*

*Refer to NPO-21046, volume and number of this NASA Tech Briefs issue, and the page number.*









National Aeronautics and  
Space Administration